Desalination and Water Treatment
www.deswater.com
doi: 10.5004/dwt.2021.27234

226 (2021) 223–241
June

Thermal and chemical pretreatment of *Cassia sieberiana* seed as biosorbent for Pb^{2+} removal from aqueous solution

Samson Ifeanyi Eze, Michael Onyema Ogbuehi, Hillary Onyeka Abugu*, Lilian Chinenye Ekowo

Department of Pure and Industrial Chemistry, University of Nigeria, Nsukka, Nigeria, Tel. +2348038847309; email: hillary.abugu@unn.edu.ng (H.O. Abugu), Tel. +2348109710052, email: michaelwealth96@gmail.com (M.O. Ogbuehi); Tel. +2348035374405; email: Eze.samson@unn.edu.ng (S.I. Eze), Tel. +2348066262080; email: chinenye.ekowo@unn.edu.ng (L.C. Ekowo)

Received 23 July 2020; Accepted 14 March 2021

ABSTRACT

Activated carbons obtained from *Cassia sieberiana* were studied for the adsorption of Pb^{2+} from an aqueous solution. Characterization of the activated carbon by Fourier-transform infrared spectroscopy (FTIR), Brunauer–Emmett–Teller, point of zero charge, thermogravimetric analysis (TGA), and scanning electron microscopy (SEM) were performed on the unmodified *Cassia sieberiana* (UMCS), thermally modified *Cassia sieberiana* (TMCS) and base modified *Cassia sieberiana* (BMCS) adsorbents. The well-known batch sorption isotherm models such as Langmuir, Freundlich and Temkin were tested with experimental data for the adsorption of Pb^{2+} to estimate the adsorption equilibrium parameters (rate constant and, adsorption capacity). The model with the best fit was identified from extensive statistical analysis of the results of nonlinear fitting of the experimental data. The FTIR analysis before and after adsorption studies confirmed the presence of different functional groups as well as shifting of functional groups after the adsorption of Pb^{2+}. SEM analysis showed the surface morphology of the different adsorbents being relatively rough and irregular indicating higher pores on the surface of the modified adsorbents. The modified *C. sieberiana* showed a large surface area (471.521, 624.772 and 628.585 m^2/g) and a point of zero charge at 4.42, 7.22 and 7.23 for UMCS, TMCS and BMCS, respectively. TGA analysis showed that the thermal decomposition of the adsorbents took place in three or less well-evidenced stages, with significant mass losses. The Langmuir isotherm gave the best fit with determination coefficients (R^2) of 1. The adsorption of Pb^{2+} ion onto UMCS, TMCS and BMCS best fitted into pseudo-second-order model with R^2 0.999 suggesting chemical adsorption mechanism. The overall adsorption process was controlled by one or more steps such as external diffusion, pore diffusion, surface diffusion and adsorption on the pore surface or a combination of more than one step as predicted by the intraparticle diffusion model. In general, modified *C. sieberiana* seed as an adsorbent can be used as an effective material for the removal of Pb^{2+} from an aqueous solution.

Keywords: Adsorbents; *Cassia sieberiana*; Biosorbents; Pb^{2+}; Chemosorption; Intraparticle diffusion model; Point of zero charge

1. Introduction

Toxic metal ions released into the environment have been on the increase due to the continuous development of electroplating, smelting, battery-making, mining and other industries [1,2]. Toxic metal ions accumulate in the food chain and living tissues, causing various diseases and disorders [3], because of their toxic, non-degradable and often deposited in organisms [4]. An increase in Pb^{2+} level leads to a higher probability of contracting cardiovascular

* Corresponding author.

This article was originally published with an error in the list of authors. Michael Onyema Ogbuehi was missing. This version has been corrected. Please see Corrigendum in vol. 257 (2022) 320 [doi: 10.5004/dwt.2022.28657].

diseases which may lead to death [4]. In that case, there is a need to develop adsorbents materials and technologies that can remove toxic metal ions from an aqueous solution.

There are many methods for the removal of toxic metal ions from industrial effluents such as chemical or electrochemical precipitation [5], ion exchange [6], adsorption on minerals and reverse osmosis [7–9]. Compared with the other processes, the adsorption of heavy metal ions from their aqueous solution onto insoluble compounds as adsorbent is the most cheapest, effective and widely used method [10]. Activated carbon is used as an adsorbent but it is expensive, and so researchers are on their toes to find cheaper and efficient alternative precursors for activated carbon production. A low-cost adsorbent is abundant, requires little processing and they are mostly waste material from industry or agriculture [11]. At present, there is growing interest in the use of modified waste materials for the adsorption of heavy metals. Unreacted plant wastes (agricultural waste) such as waste *African canarium* [12], bulk beech wood [13], papaya wood [14], maize leaf [15], teak leaf powder sago waste, banana and orange peels sawdust [16], jute fibers [3], peanut hull pellets [17], oil bean [18], maize husk [19], are inexpensive adsorbents because they have low economic value. Some of the advantages of using these biomaterials for heavy metal adsorption are simple techniques, cheap processing, high adsorption efficiency, and selective adsorption of heavy materials [11,20,21]. The adsorption efficiency has been enhanced by the pretreatment of plant wastes. Modifying agents such as base solution, acids solutions, organic compounds, oxidizing agent, dyes, etc. can extract soluble organic compounds and eliminate coloring of effluents and finally increase the efficiency of heavy metals adsorption [3,22,23]. Many studies have been carried out on the efficiency of modified low-cost adsorbents. Tarley et al. [24] reported that adsorption of Cd^{2+} increased by almost double when rice husk as a precursor was treated with NaOH. The reported adsorption capacities of Cd^{2+} were 7 and 4 mg/g for NaOH treated and unmodified rice husk respectively. Tiemann et al. [25] reported the maximum adsorption capacity of 89.2 mg/g for Pb^{2+} by NaOH-treated *alfalfa* biomass. Li et al. [23] demonstrated that Pb^{2+}, Cr^{2+} and Cu^{2+} could be effectively adsorbed by sulfuric acid-modified peanut husk. Low et al. [26] used nitric acid-modified banana peels as an adsorbent and reported the maximum capacity of 13.46 mg/g for Cu^{2+}. Karnitz et al. [27] showed that sugar cane bagasse pretreated with sodium bicarbonate could adsorb heavy metals effectively. Production of activated carbon from almond shells has been reported before. Ferro-García et al. [28] prepared three activated carbons by activation of almond shells, olive stones, and peach stones by heating in CO_2 at 1,123 K. They reported the maximum adsorption capacity of 6.65 mg/g for Zn^{2+} by almond shell carbon.

Despite the many studies about the use of plant wastes as adsorbents around the world, the literature is insufficient about the use of modified *Cassia sieberiana* as adsorbent. *C. sieberiana* seed, an agricultural waste, is from a plant native to Africa. *C. sieberiana* seed refers to seed as obtained from pods of a tropical shrub (*C. sieberiana*). *C. sieberiana*, a member of the family *Caeasalpiniaceae*, is an annual plant that grows in the world's tropical zones. It is an upright growing plant that can reach a height of more than four feet, with large, green leaves and very bright yellow flowers [29]. These seeds range in color from greenish-brown to dark brown with smooth surface and may have small bright-colored bands on the outer surface [29]. Its fruits are not edible and so litter the environment as observed in the University of Nigeria, Nsukka premises. They are used mostly for ornamental purposes because of its sharp yellowish colored leaves.

2. Materials and method

2.1. Sample collection, thermal and chemical pretreatments

C. sieberiana seed was obtained from Nsukka, Enugu State, Nigeria. The sample was identified and classified based on their botanical names by the Taxonomists in the Department of Crop Science, University of Nigeria, Nsukka. Thereafter it was washed with de-ionized water to get rid of unwanted materials. The *C. sieberiana* seed was sun-dried for several days after which it was crushed, ground and pulverized to a powdery form. The sample was then passed through a 125–300 μm mesh sieve. 0.1 g of NaOH was dissolved in 500 mL of distilled water in which 50 g of the *C. sieberiana* adsorbent was added and then mixed together by stirring. It was allowed to stand for 24 h and the excess liquid was decanted, washed with de-ionized water, dried in ovum at 110°C, stored in an air-tight container and labeled base modified *Cassia sieberiana* (BMCS). 50 g of *C. sieberiana* was carbonized in a muffle furnace at 550°C for 90 min, removed, allowed to cool, and then stored in an air-tight container already labeled thermally modified *Cassia sieberiana* (TMCS).

2.2. Adsorbate preparation

The entire chemicals used in the study were of analytical grade obtained from Sigma-Aldrich (Germany) and were used without further purification. A solution of Pb^{2+} was prepared by weighing accurately 1.598 g of $Pb(NO_3)_2$ in 50 mL of de-ionized water and was stirred properly with a glass rod. Thereafter the 50 mL solution was placed in a 1 L volumetric flask and made up to mark with de-ionized water to obtain a stock solution of 1,000 mg/L Pb^{2+}. 600 mg/L of the metal ion $Pb(NO_3)_2$ was prepared from the stock solution through serial dilution.

2.3. Adsorption study

2.3.1. Contact time

0.2 g of the adsorbent, (NaOH modified and thermally modified *C. sieberiana* seed) were placed in 100 mL plastic bottles (five for each). 20 mL of 600 mg/L of Pb^{2+} were added to each of the plastic bottles, agitated for 2 min and left to stand at different contact times of 10, 20, 30, 40, and 90 min. At the end of the given contact time for each experiment, the solution was filtered and the concentration of metal ions remaining in the filtrate was determined using atomic absorption spectrophotometer (AAS) AA-7000 Series Shimadzu (Japan).

2.3.2. Percentage removal and adsorption capacity

The percentage of Pb^{2+} removal and the adsorption capacity of the adsorbent were calculated using Eqs. (1) and (2) respectively.

$$\text{Removal}\left(\%\right) = 100\frac{\left(C_0 - C_e\right)}{C_0} \tag{1}$$

$$q_e\left(\frac{\text{mg}}{\text{g}}\right) = V\frac{\left(C_0 - C_t\right)}{m} \tag{2}$$

where q_e (mg/g) is the adsorption capacity of the adsorbents, C_0 (mg/L) is the initial metal ion concentration in solution, C_e (mg/L) is the equilibrium of the metal ion concentration, V (L) is the volume of adsorbate and m is the mass (g) of the adsorbent.

2.4. Kinetic studies

Adsorption kinetic models were applied to the experimental data in order to analyze the rate of adsorption and possible adsorption mechanism of Pb^{2+} onto unmodified *Cassia sieberiana* (UMCS), TMCS and BMCS. The pseudo-first-order model also known as the Lagergren equation is expressed as Eq. (3):

$$q_t = q_e\left[1 - \exp\left(K_1 t\right)\right] \tag{3}$$

where q_t and q_e are the amounts of metal ions adsorbed at time t and at equilibrium in (mg/g), respectively. K_1 is the pseudo-first-order adsorption rate constant (min^{-1}) [30]. Nonlinear fitting using OriginPro9 of the plots of $\log(q_e - q_t)$ vs. t were used to determine the rate constant (K_1) and q_e.

The pseudo-second-order kinetic model was also used to test the kinetic data obtained from the adsorption of Pb^{2+} onto UMCS, TMCS and BMCS [Eq. (4)].

$$q_t = \frac{\left(q_e^2 K_2 t\right)}{1 + K_2 q_e t} \tag{4}$$

where K_2 is the equilibrium rate constant of pseudo-second-order adsorption (L/mg min) [31]. The values of q_e and K_2 were calculated using the nonlinear plot of t/q_t against t [31,32]. The initial sorption rate, h (mg/L min), was also calculated from Eq. (5).

$$h = K_2 q_e^2 \tag{5}$$

The intraparticle diffusion model by Weber and Morris [33] was applied to predict the rate–limiting step in the adsorption of Pb^{2+}. For a solid–liquid sorption process of this nature, the solute transfer is usually characterized by external mass transfer (boundary layer diffusion), intraparticle diffusion or both. The intraparticle diffusion model equation is given as Eq. (6).

$$q_t = K_{\text{id}} t^{0.5} + C \tag{6}$$

where q_t = adsorption at time t, K_{id} = intraparticle diffusion rate constant (mg/g $\text{min}^{1/2}$) and C = constant that gives the thickness of the boundary layer, that is, the larger the values of C, the greater the boundary layer effects. A plot of q_t vs. $t^{0.5}$ gives a straight line from the origin for the sorption process to be controlled by intraparticle diffusion.

2.5. Error analysis

Two error functions of non-linear regression basis were examined in order to evaluate the fit of the kinetic models to represent the experimental data [34,35]. The Hybrid Fractional Error Function (HYBRID), which is given as Eq. (7):

$$\text{HYBRID} = \frac{100}{n-p}\sum\left[\frac{\left(q_{e,\text{exp}} - q_{e,\text{cal}}\right)}{q_{e,\text{exp}}}\right]^2 \tag{7}$$

Marquardt's Percent Standard Deviation (MPSD) error function which is also given as Eq. (8):

$$\text{MPSD} = 100\sqrt{\frac{1}{\left(n-p\right)}\sum\left[\frac{q_{e,\text{exp}} - q_{e,\text{cal}}}{q_{e,\text{exp}}}\right]^2} \tag{8}$$

where $q_{e,\text{exp}}$ = experimental equilibrium adsorption capacity, $q_{e,\text{cal}}$ = theoretical equilibrium adsorption capacity, n = number of experimental data points and p = the number of parameters in each isotherm model. HYBRID was developed to improve the fit of the square of errors function at low concentration values while the MPSD is similar in some respects to a geometric mean error distribution modified according to the number of degrees of freedom of the system.

2.6. Brunauer–Emmett–Teller surface area and point of zero charge

The Brunauer–Emmett–Teller (BET) surface area was obtained by the Quantachrome NovaWin Version 11.03 Model Analyzer while the point of zero charge (PZC) was obtained using acid-base potentiometric titration method according to Miyittah et al. [36]; Uehara and Gillman [37]. Briefly, about 4 g of the sample was weighed into 20 mL of 0.002 M KCl and the mixture was equilibrated for about 24 h through shaking. The initial pH of the suspensions was varied using 0.1 M HCl and 0.1 M NaOH while the blank contained no acid or base. The pH of suspensions was measured after each subsequent addition and equilibration with 0.1 M (1 mL) KCl and 2 M (0.5 mL) KCl. The amount of potential-determining ions (H^+/OH^-) adsorbed was estimated as the pH difference between the blank and acid/base titrated suspensions at each different KCl concentration.

3. Results and discussion

3.1. Characterization of the biosorbents

3.1.1. Fourier-transform infrared spectroscopy

Functional group types and net charge bonded to the carbon surface is essential in understanding the mechanism

of adsorption of ionic adsorbates on activated carbons [38]. The adsorption capacity of activated carbon is influenced by functional groups on the carbon surface. Functional groups do not only affect the adsorption behavior but also dominate the adsorption mechanism. While increasing the uptake kinetics at a lower coverage (monolayer coverage), they also reduce the binding energy [39].

The Fourier-transform infrared spectroscopy (FTIR; Shimadzu 8300, Japan and Agilent 4500, USA) spectra of UMCS, TMCS and BMCS were recorded in the range of 4,000–400 cm^{-1} (Figs. 1–6). The spectra identified the surface functional groups and also illustrated the changes in the biosorbent after thermal and base modification treatments. The unmodified *C. sieberiana* spectrum (Fig. 1) exhibits several bands of multiple intensities merged to form a broad and strong band in the functional group region of 3,410 cm^{-1}, which is associated with the stretching vibrations of free or bonded OH groups of alcohols and carboxylic acids. In the loaded unmodified biosorbent (Fig. 2), the OH shifted to 3,268 cm^{-1}. Also, with the presence of inter and intra-molecular hydrogen bonding between these hydroxyl groups which is in accordance with the results of Bojić et al. [40], 2,359 cm^{-1} peak indicated the presence of amines (RNH_2) [41], which was conspicuously missing in the loaded UMCS. The peak at 2,928 cm^{-1} vibration frequency of the unmodified *C. sieberiana* indicated the presence of C–H bond and terminal alkynes, while the vibration frequency at 1,651 cm^{-1} shows the presence of carbon–carbon bond. The loaded UMCS also gave C–H at 2,929 cm^{-1}, but the C=C at 1,651 cm^{-1} shifted to 1,629 cm^{-1}. Hu et al. [42], in Pb^{2+} biosorption from aqueous solutions by live and dead biosorbents of the hydrocarbon-degrading strain *Rhodococcus* sp. HX-2, attributed peaks at 2,929.75 and 2,863.31 cm^{-1} to the stretching vibration of the $–CH_2$ group, and those at 1,664.49 and 1,542.98 cm^{-1} to the stretching vibration of the –NH and –CN groups, respectively. The spectra intensities merged to form a broad and weak band in the functional group's region of 1,074 and 1,030 cm^{-1} which suggested an asymmetric stretching vibration of alkane chains example, CH_4 [43]. Other functional groups present in the loaded UMCS are C–O of COOH, ethers, alcohols or esters (1,060–1,030 cm^{-1}) and C–H of alkanes (1,413–1,380 cm^{-1}). But in the unloaded UMCS, these functional groups shifted to different spectra, while others were missing.

The unloaded TMCS (Fig. 3) show C–H band of C=C–H (alkanes or aromatic compound) at 1,421–1,462 cm^{-1}, C–N or C–O of aromatic rings at 1,007 cm^{-1}, C–H of alkenes at 698–877 cm^{-1}, C–H of alkanes at 2,948–3,018 and C=O of ketones, aldehyde, COOH or esters at 1,700–1,719 cm^{-1}. But the loaded thermally modified *C. sieberiana* FTIR (Fig. 4) show OH of alcohol, C–H of alkanes, C–O of carboxylic, ester, ethers or alcohol at 3,217.37, 2,972.40, and 1,016.52 cm^{-1} adsorption band respectively. Jha and Jha [44], obtained a similar results in the iodine adsorption by activated carbon of modified *Spinacia oleracea* (spinach) leaves.

The band at 3,450.77 cm^{-1} of the unloaded BMCS (Fig. 5) show the OH group of carboxylic acids, while 2,928.04, 1,651.12, 1,058.96–1,028.09 and 1,151.54 cm^{-1} showed the C–H of alkanes, C=C of alkene, C–O of esters, COOH, ethers or alcohol and C–N of amines or amides respectively. In the FTIR of the loaded BMCS biosorbent (Fig. 6), there was shifting of these observed bands and formation of new ones (Nitrate ion at 1,380 cm^{-1}, N–H bend of secondary or primary amine at 1,622 cm^{-1}). This showed that base treatment had significant effects on the functional groups. The hydroxyl and carboxylic groups present on the surfaces of both the biosorbents are believed to clearly act as an active site for binding of positively charged cations in line with the findings of Kirova et al. [45].

3.1.2. Scanning electron microscopy

Figs. 7–9 shows the scanning electron microscope (Shimadzu ESCA-750, Japan) image of UMCS, TMCS and BMCS respectively. The surface morphology of the UMCS, TMCS and BMCS were studied, aimed at visualizing the

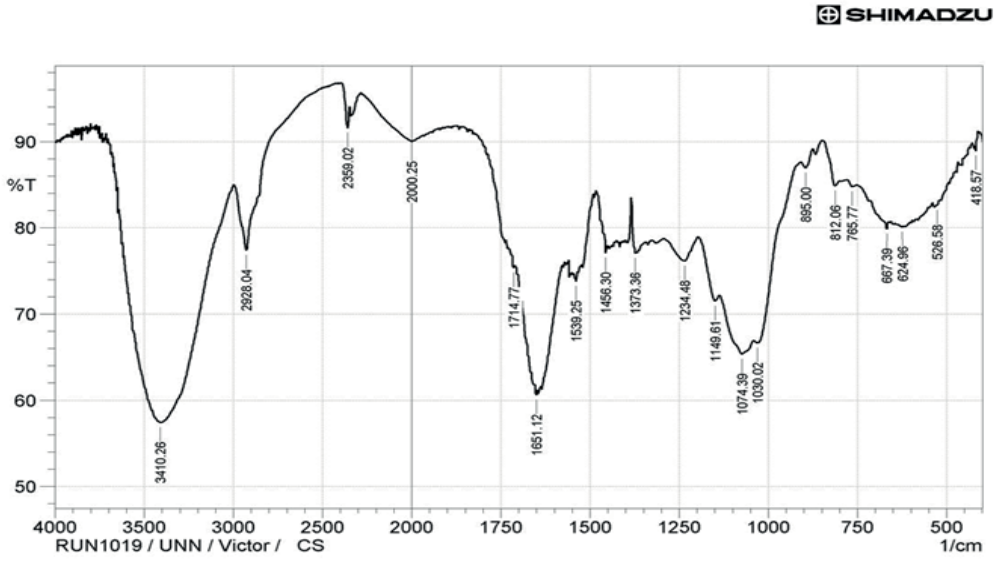

Fig. 1. FTIR spectrum of unmodified *Cassia sieberiana*.

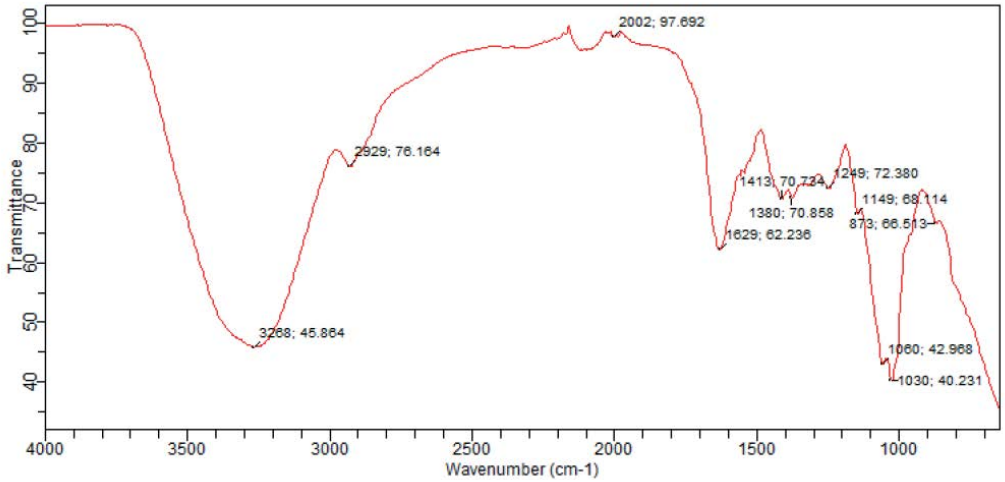

Fig. 2. FTIR spectrum of unmodified *Cassia sieberiana* after adsorption study (loading).

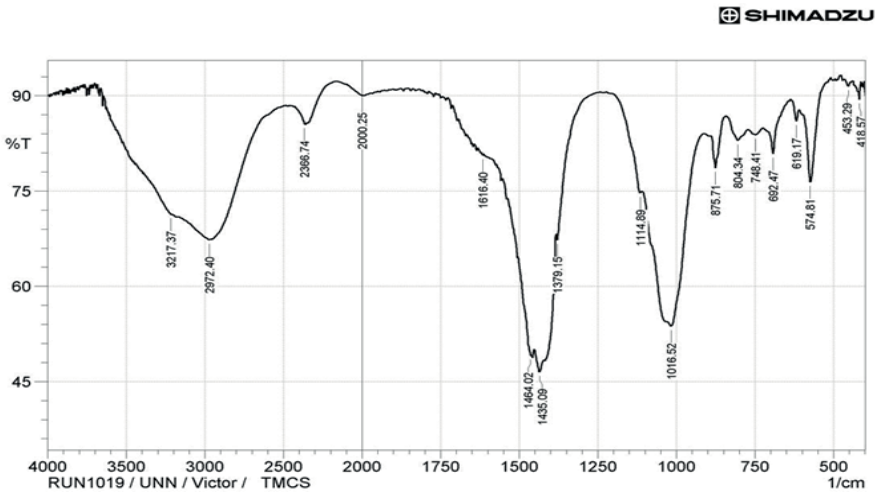

Fig. 3. FTIR spectrum of thermally modified *Cassia sieberiana*.

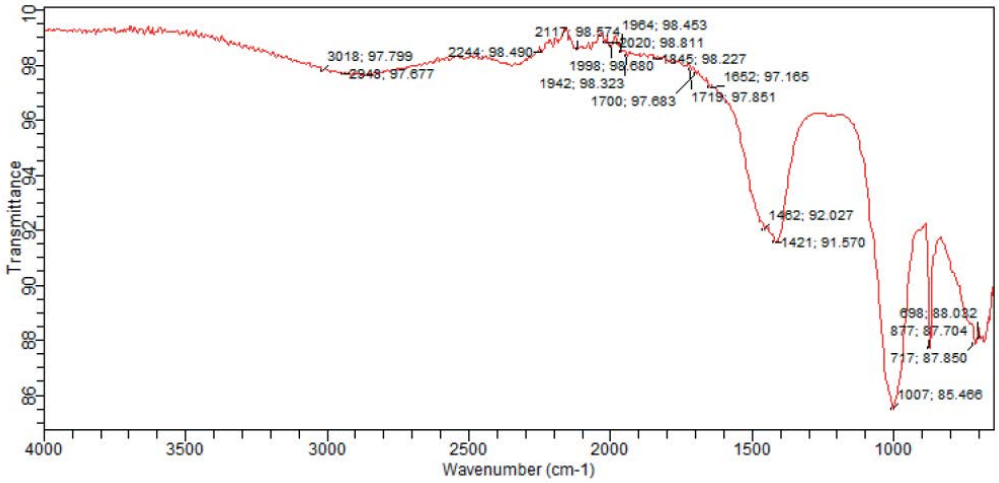

Fig. 4. FTIR spectrum of thermally modified *Cassia sieberiana* after adsorption study (loading).

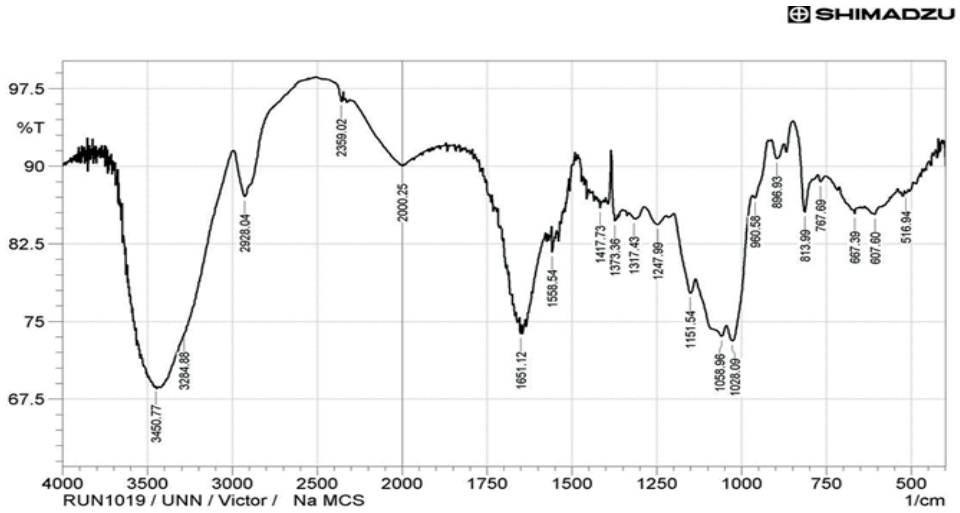

Fig. 5. FTIR spectrum of base (NaOH) modified *Cassia sieberiana*.

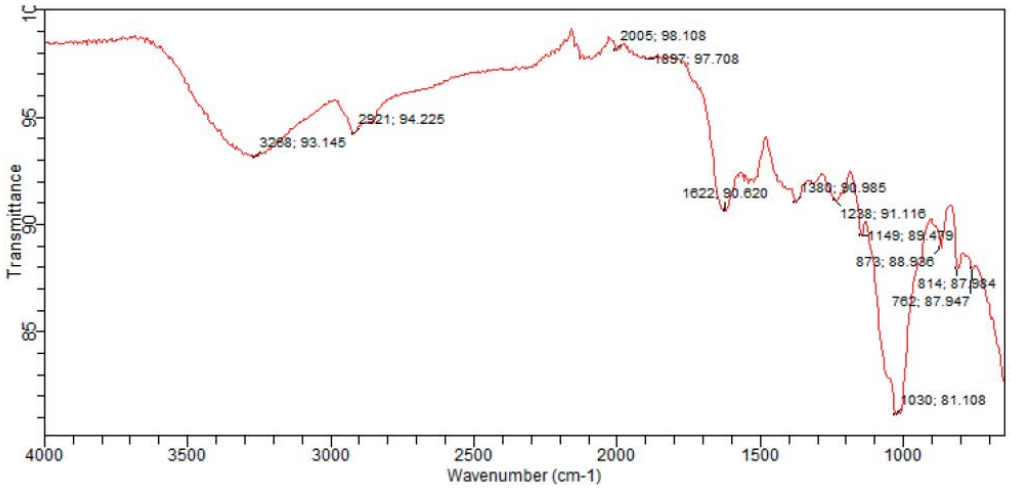

Fig. 6. FTIR spectrum of base (NaOH) modified *Cassia sieberiana* after adsorption study (loading).

morphological characteristics obtained from the activation process at different modification conditions. From the micrographs, pores are evident on the surface of the prepared activated *C. sieberiana*. The UMCS appeared to have a fairly smooth surface with cracks or voids, while the TMCS and BMCS were relatively rough and irregular indicating the higher pores on the surface of the modified *C. sieberiana*. This showed that the activation stage produced extensive external surfaces with quite irregular cavities and pores. The high porosity observed on the surface of the modified *C. sieberiana* were as a result of burn-offs from the surface, pores of *C. sieberiana* and base evaporation leaving voids. This is in line with Hesas et al. [46] observation in the methylene blue adsorption by activated carbon from apple waste.

3.1.3. Thermogravimetric analysis

The thermogravimetric analysis (Perkin Elmer TGA-7, United Kingdom) pattern of UMCS, TMCS and BMCS are shown in Figs. 10–12, respectively. From the figures, it was observed that the adsorbents were thermally stable up to temperature of 520°C, 510°C, and 450°C for UMCS, TMCS and BMCS, respectively.

According to the TGA curves, the thermal decomposition of all adsorbent types under investigation took place in three or less well-evidenced stages, with significant mass losses, but the loss of mass accompanying them is quite different and takes place in much narrower temperature ranges. The initial mass loss from 0°C to 300°C is attributed to the adsorbed moisture since the *C. sieberiana* husk was hitherto dried at about 110°C for 1 h. The second mass loss step from 300°C to about 450°C is attributed to the thermal degradation of hemicellulose and cellulose, forming a carbonaceous residue from 450°C which decomposes slowly up to about 520°C. The final residue formed was about 10%–15%, which is consistent with a mixture of ash and carbon. This is in line with the observation of Oliveira et al. [47] in the TGA/DTA analysis of renewable biomass,

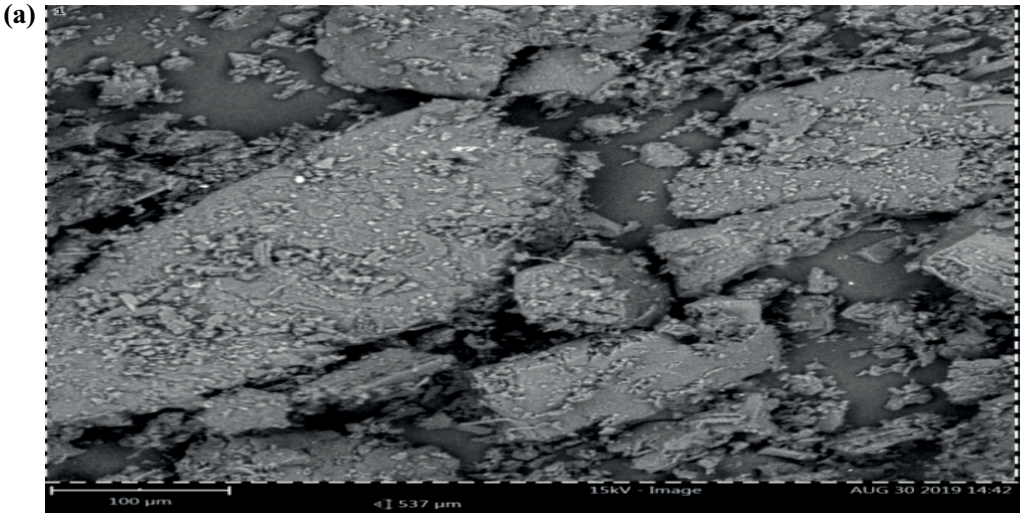

Fig. 7. SEM image and elemental content of unmodified *Cassia sieberiana* (at 100 to 537 µm).

babassu. Bazan et al. [48] in the thermal analysis of activated carbon obtained from the residue after supercritical extraction of hops.

3.2. Effect of contact time

The effect of contact time on the adsorption of Pb^{2+} onto UMCS, TMCS and BMCS is as shown in Fig. 13. The adsorption process decreased gradually between 10 to 20 min for UMCS, and then decreased sharply from 20 to 30 min. There was a significant rapid increase in adsorption from 30 to 40 min and then diminished gradually for the next 50 min.

For the adsorption of Pb^{2+} onto TMCS, a gradual decrease in adsorption was observed for 30 min and also a gradual increase for the next 15 min. After 40 min there was no significant increase in adsorption (Fig. 14). In the adsorption of Pb^{2+} onto BMCS, a rapid decrease was observed from 97% to 93% for 10–20 min and a rapid increase from 93% to 95% for the next 10 min. However, a sharp decrease in adsorption is observed from 94.83% to 91.38% for the next 10 min. Then from 40 to 90 min, there is no significant change or increase in adsorption. A gradual and rapid decrease for both UMCS and BMCS showed that the adsorption site has been filled up at 40 min and consequently became saturated attaining equilibrium (Fig. 14). This is in agreement with Gupta et al. [49] observation in the removal of lead and chromium from aqueous solution using red mud-an aluminum industry waste. Equilibrium was established around 40 min for both UMCS and BMCS but about 45 min for TMCS. The sorption that rapidly occurs in both UMCS and BMCS is normally controlled by the diffusion process from the bulk of the solution to the adsorbent surface [50]. The slow uptake in the later stages is probably due to an attachment-controlled process caused by less available active sites for sorption in accordance with the findings of Argun et al. [51] in the toxic metal ions adsorption by modified oak sawdust.

3.3. Adsorption isotherm

3.3.1. Langmuir isotherm

The Langmuir isotherm is used to describe adsorption based on the assumption that uptake occurs on a homogenous surface by monolayer sorption without interaction

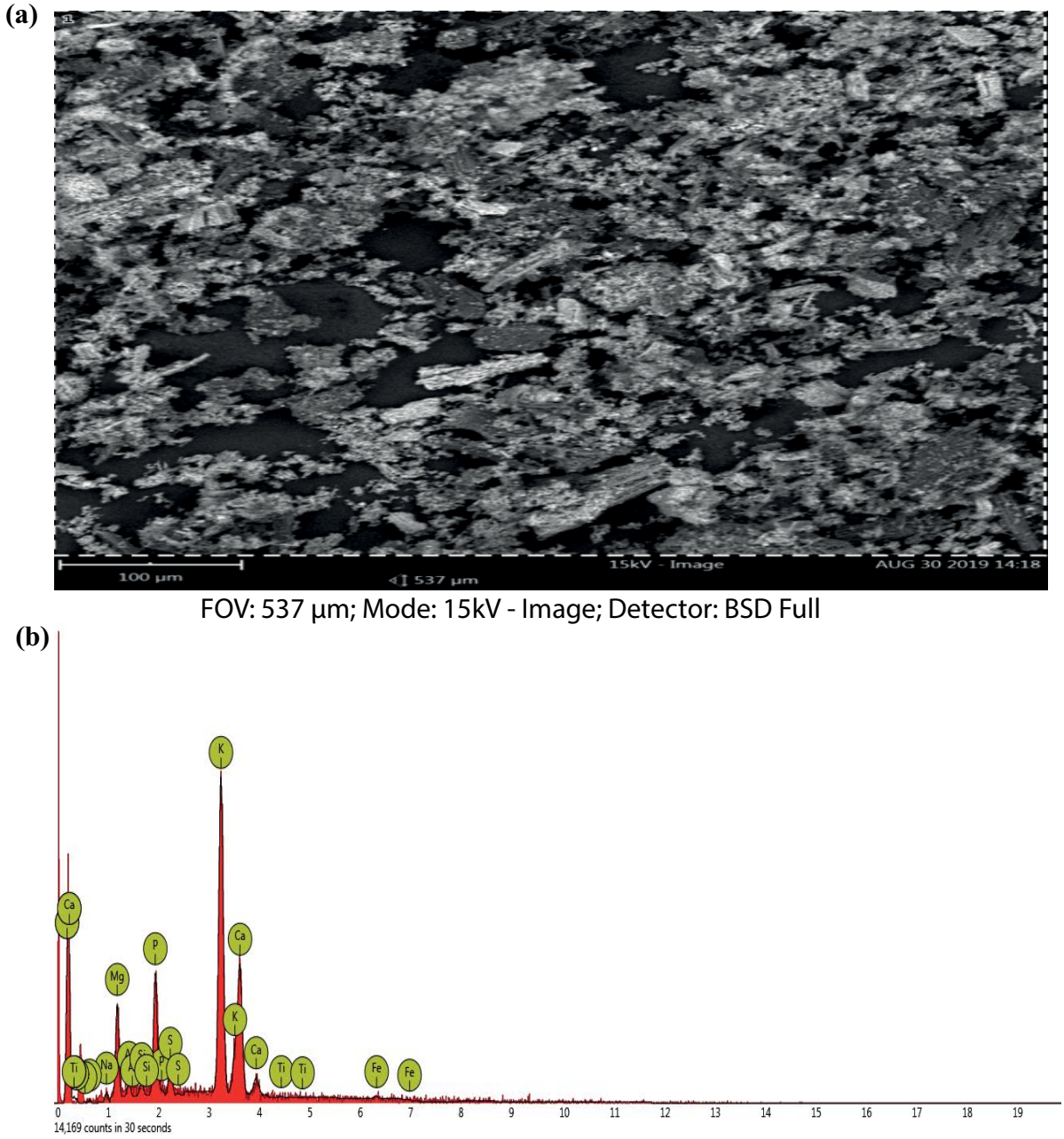

Fig. 8. SEM image and elemental content of thermally modified *Cassia sieberiana* (at 100 to 537 µm).

between adsorbed molecules. The nonlinear form of the Langmuir isotherm equation can be expressed as Eq. (9):

$$q_e = \frac{\left(q_m K_L C_e\right)}{\left(1 + K_L C_e\right)} \tag{9}$$

where q_e is the monolayer adsorption capacity of the adsorbent (mg/g), K_L is the Langmuir adsorption constant (L/mg) related to the energy of adsorption, which quantitatively reflects the affinity between the adsorbent and the adsorbate, q_m is the maximum monolayer adsorption capacity of the adsorbent (mg/g). The constant q_m and K_L can be determined from the slope and the intercept of the linear plot of C_e/q_e and C_e. The Langmuir isotherm plot for the adsorption of Pb^{2+} onto UMCS, TMCS and BMCS (Fig. 15), showed excellent fit.

3.3.2. Freundlich isotherm

The Freundlich isotherm model assumes a multilayer adsorption onto a heterogeneous adsorbent surface and provides the exponential distribution of the active sites. The nonlinear form of Eq. (10) is:

$$q_e = K_F C_e^{1/n} \tag{10}$$

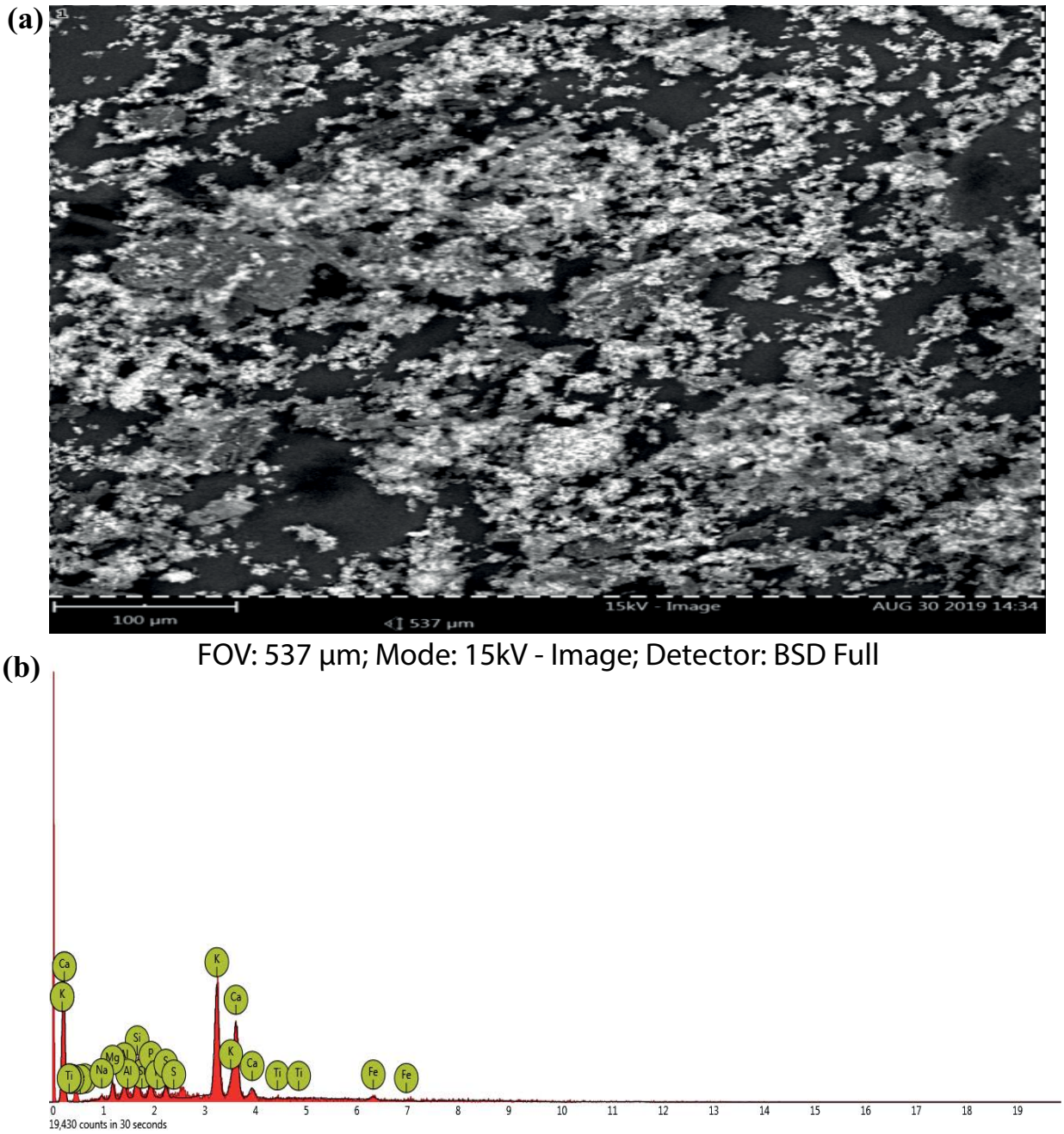

Fig. 9. SEM image and elemental content of NaOH modified *Cassia sieberiana* (at 100 to 537 µm).

where K_F (mg/g)(mg/L)$^{1/n}$ and n is the Freundlich adsorption constant related to the adsorption capacity and the intensity of the adsorbents respectively. The constants were determined by the nonlinear plot of logq_e vs. logC_e using OriginPro9 (Fig. 16). The determination coefficient (R^2) of Pb^{2+} adsorption fell within 0.997–1 indicating a good fit (Table 1). The results obtained were satisfactory with the given experimental data. This suggests that apart from homogeneous adsorption behavior as inferred from Langmuir's model, the availability of heterogeneous adsorption sites or possibilities of surface interaction (chemical interaction) between the adsorbate and the adsorbent could be possible. This is in agreement with the experimental results obtained by Swapna Priya and Radha [52] in the adsorption studies of tetracycline hydrochloride onto commercial-grade granular activated and Das and Mondal [50] in the calcareous soil as a new adsorbent to remove lead from aqueous solution.

3.3.3. Temkin isotherm

The Temkin isotherm model takes into account the interactions between adsorbents and metal ions to be adsorbed and is based on the assumption that the free

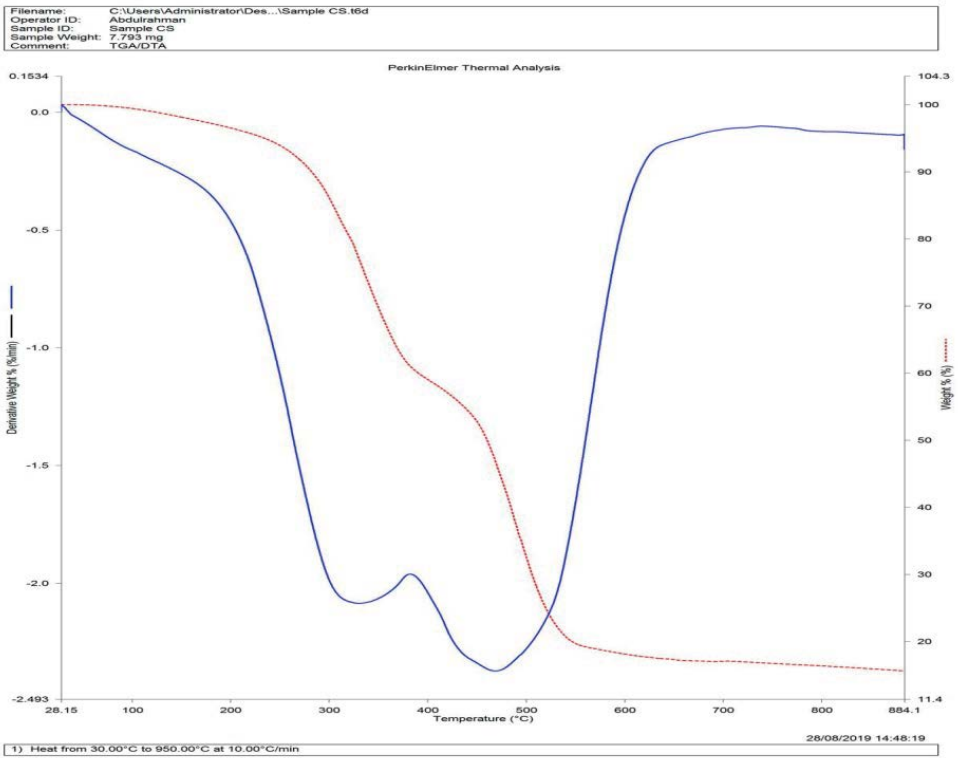

Fig. 10. Thermal gravimetric analysis of unmodified *Cassia sieberiana*.

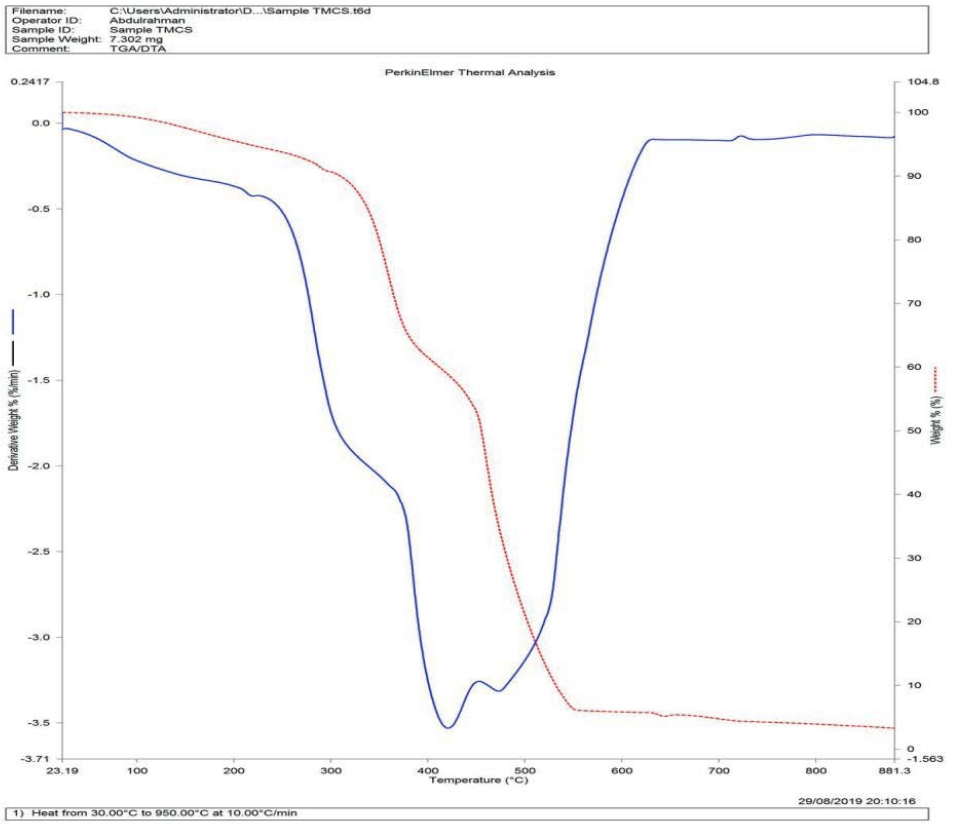

Fig. 11. Thermal gravimetric analysis of thermally modified *Cassia sieberiana*.

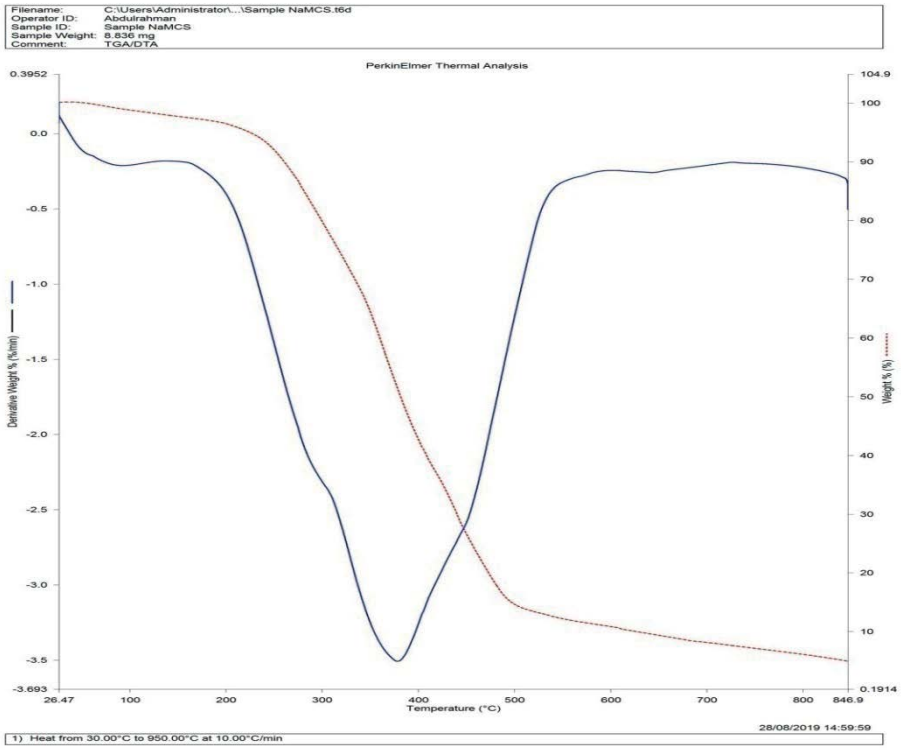

Fig. 12. Thermal gravimetric analysis of base modified *Cassia sieberiana*.

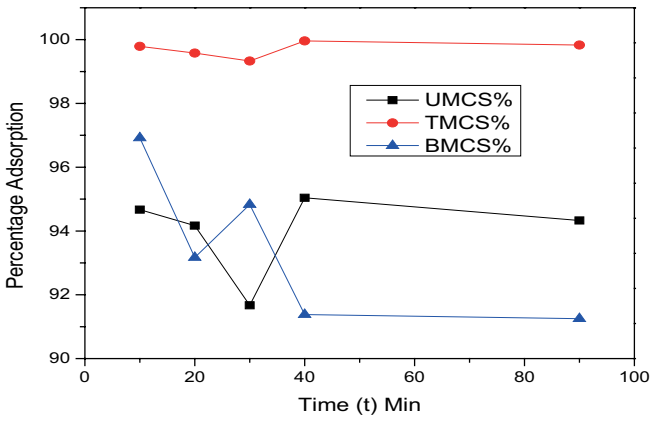

Fig. 13. Effect of contact time on the percentage adsorption of Pb^{2+} onto UMCS, TMCS and BMCS *Cassia sieberiana* seed.

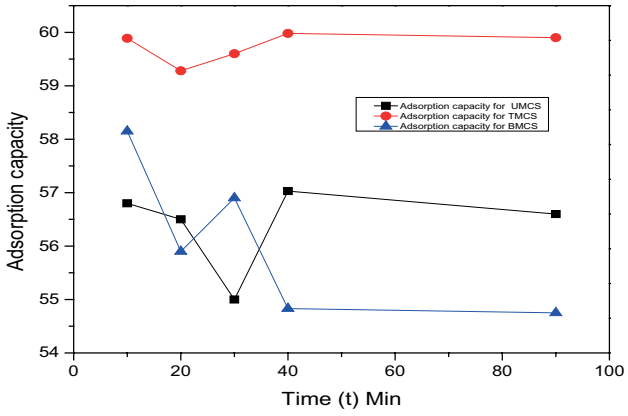

Fig. 14. Effect of contact time on the adsorption uptake of Pb^{2+} onto unmodified, thermally modified and base modified *Cassia sieberiana*.

energy of adsorption is a function of the surface coverage. The nonlinear form of the Temkin isotherm model is expressed as:

$$q_e = \frac{RT}{b}\ln\left(K_T C_e\right) \tag{11}$$

$$q_e = B\ln\left(K_T C_e\right) \tag{12}$$

where $B = RT/b$, T is the temperature (K), R is the ideal gas constant (8.314 J/mol K), q_e is the adsorption capacity at equilibrium (mg/g), C_e is the equilibrium concentration of adsorbate in the bulk solution (mg/L), B is the Temkin constant related to the heat of adsorption or the maximum binding energy (J/mol). The Temkin plot of q_e vs. $\ln C_e$ (Fig. 17) for the adsorption of Pb^{2+} onto UMCS, TMCS and BMCS showed a determination coefficient (0.544 to 0.9999) to be a relatively good data fit. Temkin model equation was derived on the assumptions that adsorption sites are similar owing to the impact of the substance adsorbed at the adjacent sites and that the energy of adsorption decreases directly with an increase in active site coverage [53]. When all the active sites are used, the

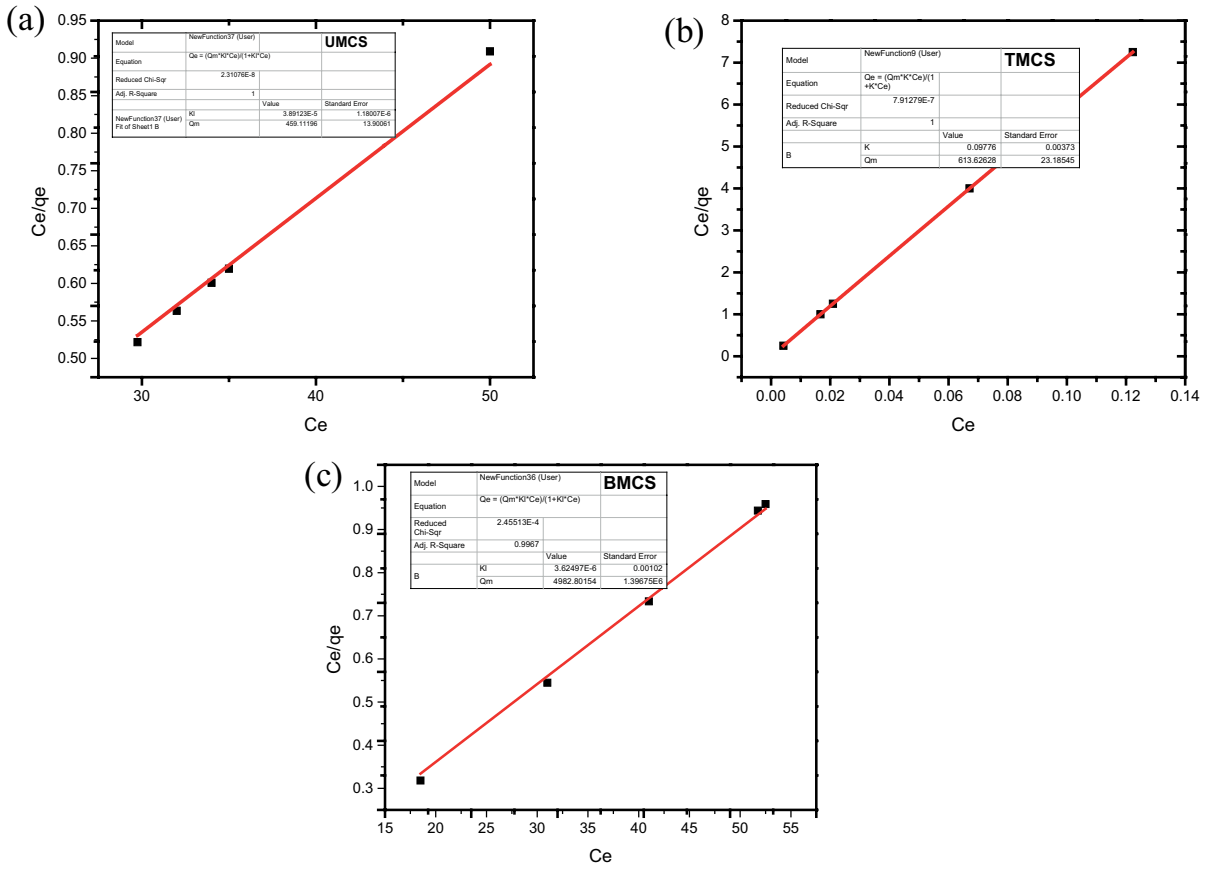

Fig. 15. Langmuir isotherm plot for the adsorption of Pb^{2+} onto UMCS (a), TMCS (b) and BMCS (c).

Table 1
Langmuir, Freundlich and Temkin isotherm constants for Pb^{2+} adsorption onto UMCS, TMCS and BMCS

Isotherm models	UMCS	TMCS	BMCS
	Langmuir model		
q_m (mg/g)	459.11 ± 13.9	613.63 ± 23.19	4,982.80 ± 1.39E-6
K_L (L/mg)	3.89E-5 ± 1.18E-5	0.097 ± 0.0037	3.625 ± 0.00102
R^2	1.000	1.000	0.997
	Freundlich model		
K_F (mg/g)(mg/L)$^{1/2}$	1.8011 ± 0.0024	1.775 ± 6.83E-19	1.787 ± 0.00459
n	0.0644 ± 0.003	6.84E-4 ± 2.5E-19	0.0488 ± 0.00568
R^2	0.991	1.000	0.947
	Temkin model		
B (mg/g)	–14.577 ± 0.657	–0.861 ± 0.575	–10.174 ± 4.235
K_T	0.00585 ± 0.00102	3.92E-31 ± 8.9E-29	0.00114 ± 0.0026
R^2	0.991	0.073	0.544

distribution of energy is uniform along the length of the active site's coverage and in addition to this, the coverage neither approaches zero or unity. As this model explains the multivalent surface interactions of the adsorbate onto the surface of the adsorbent, the high correlation values obtained show that surface interactions between adsorbents and Pb^{2+} may possibly be the dominant process in the adsorption of Pb^{2+} onto the surface of *C. sieberiana*. This result is in agreement with the results obtained by Dada et al. [54] in phosphoric acid modified rice husk.

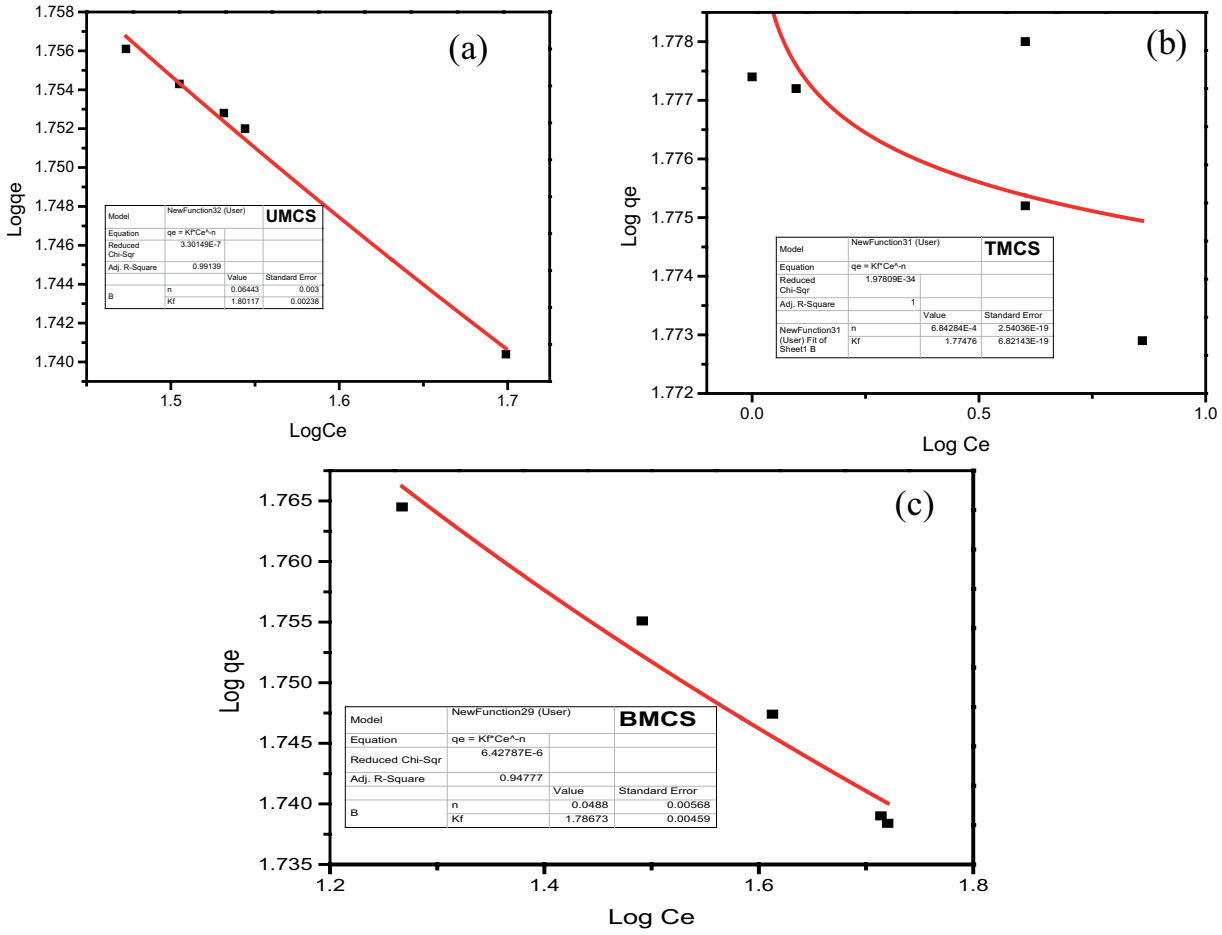

Fig. 16. Freundlich isotherm plot for the adsorption of Pb(II) ion onto UMCS (a), TMCS (b) and BMCS (c).

The nonlinear plots of the adsorption isotherm data (Table 1), showed that the Langmuir monolayer adsorption capacity q_m ranged from 459.11 to 4,982.80 mg/g for the biosorbents with BMCS having the best adsorption capacity. Freundlich and Temkin's model was not suitable to describe Pb^{2+} adsorption on these modified *C. sieberiana*. The B values of Temkin adsorption isotherm for UMCS, TMCS and BMCS were very low indicating an increase in active site coverage. With these results, it can be inferred that Langmuir adsorption isotherm best describes the adsorption of Pb^{2+} onto *C. sieberiana*, suggesting homogeneous surface adsorption by monolayer sorption without interaction between sorbed ions.

The pseudo-first-order equation did not fit into the experimental data of Pb^{2+} ion adsorption by UMCS, TMCS and BMCS (Fig. 18). This is indicated by the low value of the determination coefficients (0.342–0.462) and the rate constant K_1. The pseudo-second-order model provides a good fit to the experimental data of Pb^{2+} adsorption (Fig. 19). The R^2 values were excellent with high values of equilibrium rate constant K_2 for UMCS, TMCS and BMCS. These revealed that the pseudo-second-order model best describes the experimental data obtained from the adsorption of Pb^{2+} by UMCS, TMCS and BMCS. Therefore, the suitability of the second-order kinetics to explain the adsorption mechanism suggests chemical adsorption. This is in agreement with the results of Das and Mondal [50].

The error functions (HYBRID and MPSD) corresponding to the minimized deviations between the experimental and calculated kinetic models suggest pseudo-second-order kinetics as the best (the lowest values of the error functions) according to Sreńscek-Nazzal et al. [55] (Table 2), and this indicates that the adsorption is chemosorption. The calculated q_{e2} values were closer to the experimental q_e values suggesting the overall rate of the adsorption process to be most likely controlled by the chemosorption process and the rate of the reaction directly proportional to the number of active sites on the surface of the activated carbons [56].

The BET multipoint measurement surface area showed that BMCS (628.585 m^2/g) and TMCS (624.772 m^2/g) possessed higher specific surface area more than the UMCS (471.521 m^2/g) adsorbent (Fig. 20) showing the effect of base and thermal modifications on the *C. sieberiana* seed.

The knowledge of PZC which is the point where the total positive charges are equal to the total negative charges on adsorption surfaces plays an important role in understanding ion-sorption processes at the metal/solution interface [57]. Negatively charged surfaces are surfaces with a negative charge in physiological environments (pH 7). Such surfaces possess an isoelectric point (PI or PZC)

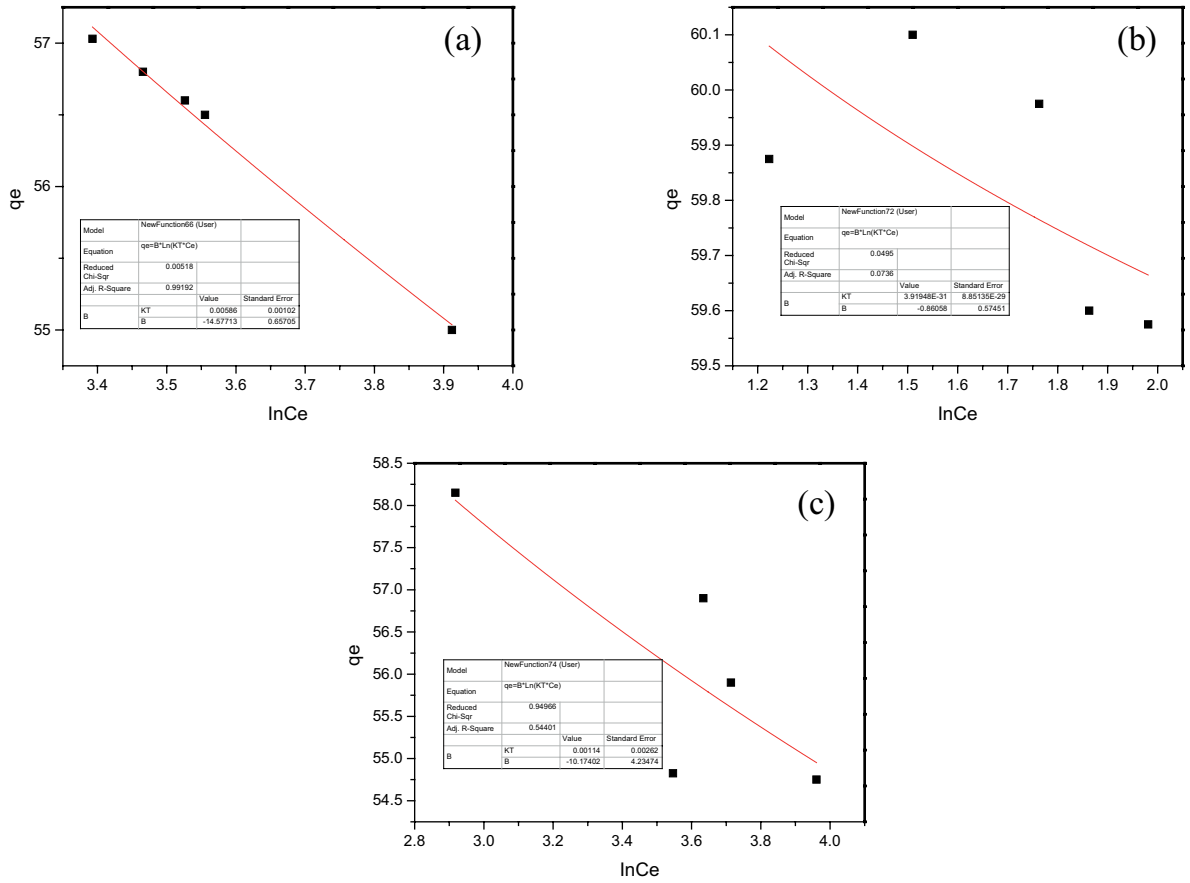

Fig. 17. Temkin isotherm plot for the adsorption of Pb(II) ion onto UMCS (a), TMCS (b) and BMCS (c).

Table 2
Comparison of the kinetic model equations on the adsorption of Pb^{2+} solution of UMCS, TMCS and BMCS

Kinetic models	UMCS	TMCS	BMCS
$q_{e,exp}$ (mg/g)	57.03	59.98	58.15
	Pseudo-first-order		
$q_{e,cal}$ (mg/g)	–0.776 ± 0.361	–1.077 ± 0.393	0.0891 ± 0.149
K_1 (min^{-1})	0.0322 ± 0.00696	0.0254 ± 0.0062	–0.0624 ± 0.135
R^2	0.462	0.466	0.342
	Pseudo-second-order		
h (mg/L min)	1.78E-02	1.67E-02	1.82E-02
K_2 (L/mg min)	6.34E-7 ± 2.4E-62	2.07E-7 ± 3.3E-7	1.822E-9 ± 1.7E-7
$q_{e,cal}$ (mg/g)	167.64 ± 293.44	284.46 ± 225.57	3,159.05 ± 148,843
R^2	0.999	0.999	0.999
	HYBRID		
First-order	34.25	34.54	33.23
Second-order	125.39	466.86	16,682
	MPSD		
First-order	33.79	33.93	33.28
Second-order	–64.65	–124.75	–745.70

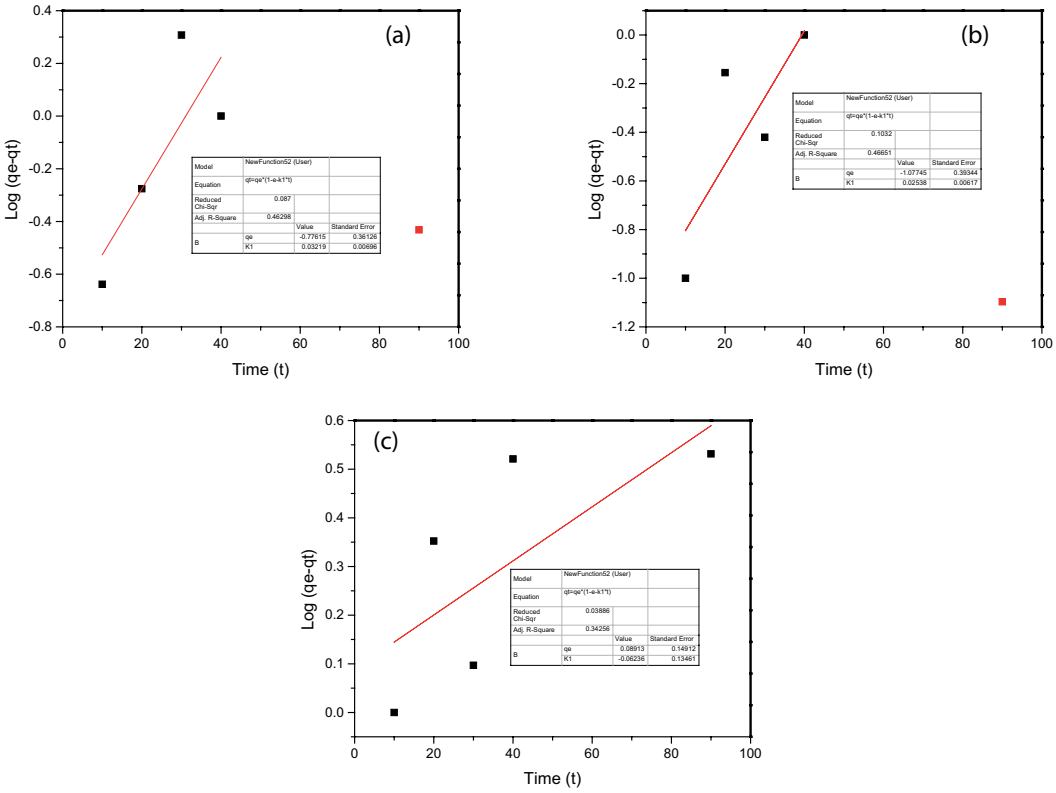

Fig. 18. Pseudo-first-order plot of Pb^{2+} onto UMCS (a), TMCS (b) and BMCS (c).

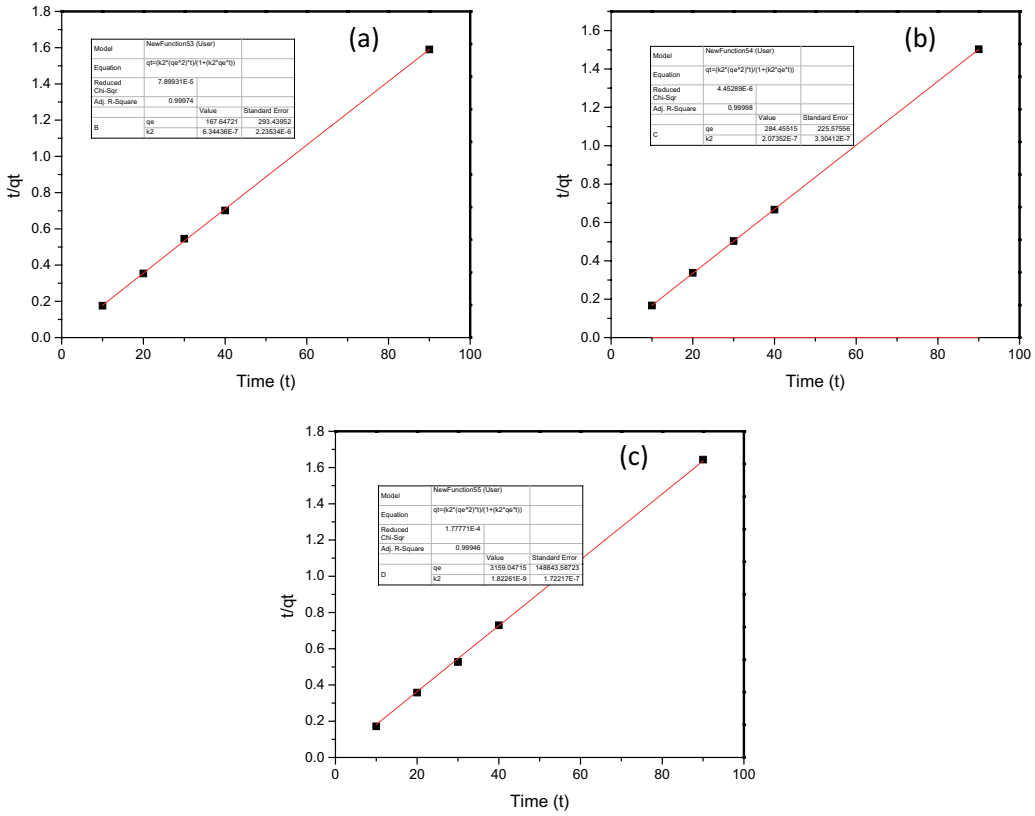

Fig. 19. Pseudo-second-order plot of Pb^{2+} onto UMCS (a), TMCS (b) and BMCS (c).

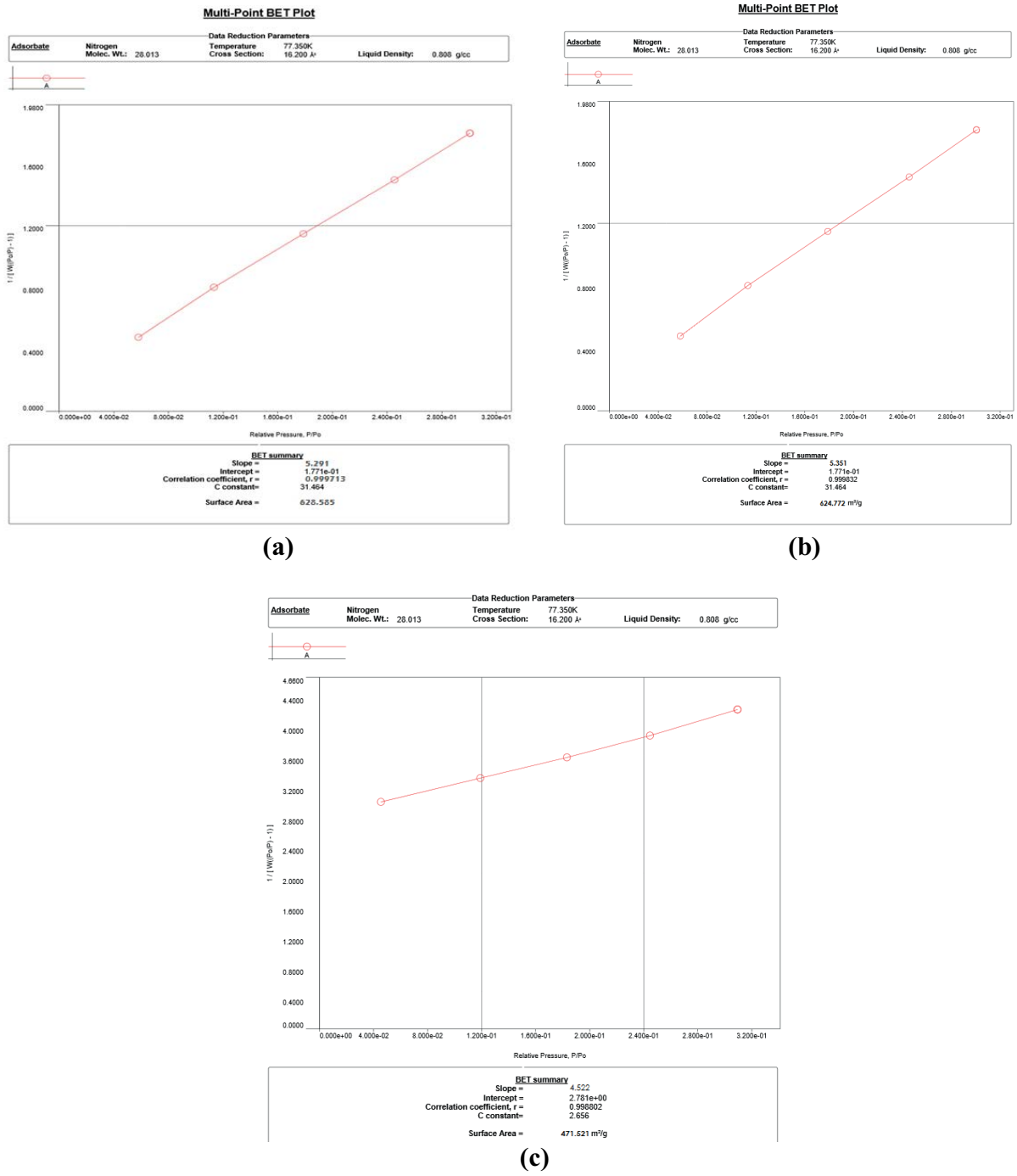

Fig. 20. BET surface area of BMCS (a), TMCS (b) and UMCS (c).

below pH 7 [57,58]. The ion affinity of this class of minerals is pH-dependent. As the pH of the solution in contact with the adsorbate solution is reduced below the point of zero charge (PZC), the surface of the adsorbate solution becomes positively charged. Conversely, as the pH is increased above the PZC, the surface becomes negatively charged. The acid-base potentiometric titration data showed the PZC of UMCS at 4.42, TMCS at 7.22 and BMCS at 7.23 (Fig. 21). The PZC of the modified *C. sieberiana* was higher than the UMCS. The PZC result obtained for the modified *C. sieberiana* (TMCS and BMCS) were comparable to the values recorded by Moon et al. [59] and Mahmood et al. [60] in the preparation of ZrO_2-coated NiO powder and comparison of different methods for the PZC determination respectively.

3.4. Prediction of rate-limiting step

The intraparticle diffusion model by Weber and Morris [33] was applied to predict the rate–limiting step in the adsorption of Pb^{2+}. For a solid–liquid sorption process of

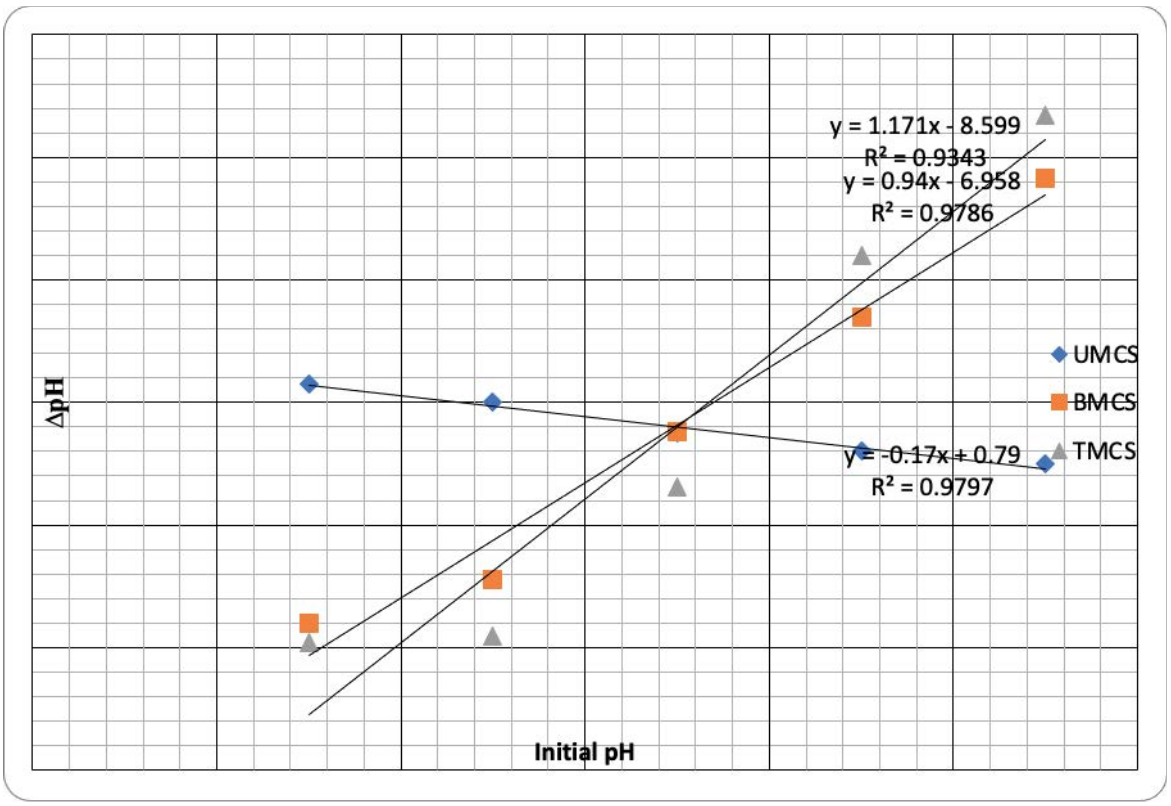

Fig. 21. Influence of varying pH at 25°C ± 2°C in determining the PZC.

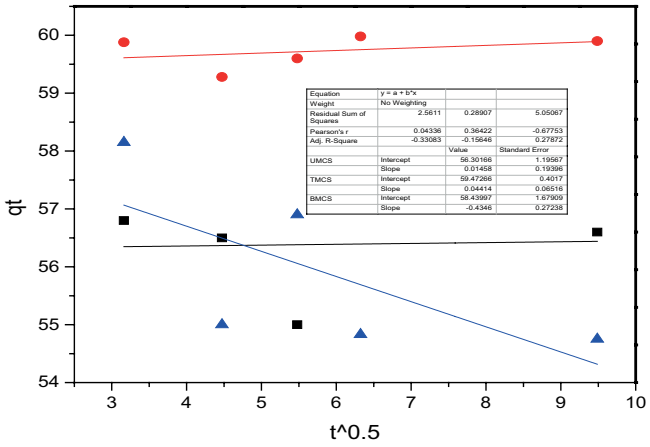

Fig. 22. Intraparticle plot of Pb^{2+} onto UMCS, TMCS and BMCS.

this nature, the solute transfer is usually characterized by external mass transfer (boundary layer diffusion), intraparticle diffusion or both. The result (Fig. 22) showed that the plot of q_t vs. $t^{0.5}$ did not give a straight line graph that starts from the origin and this suggests that intra-particle diffusion is not the only rate-limiting step involved in the adsorption of these metals on the activated carbons obtained, according to Weber and Morris [33]. The variation from the origin may be due to the variation of mass transfer in the initial and final stage adsorption according to Mohanty et al. [61]. This indicates that the overall adsorption process may be controlled either by one or more steps such as external diffusion, pore diffusion, surface diffusion and adsorption on the pore surface or a combination of more than one step.

4. Conclusion

The study successfully functionalized TMCS and BMCS from UMCS which is evidenced in the FTIR spectrum showing the groups that acted as binding sites for the adsorption of Pb^{2+}. Unmodified *C. sieberiana* seed of Nigerian origin was successfully utilized as an adsorbent for the removal of Pb^{2+} ion from an aqueous solution by batch adsorption method. The experimental factor such as the contact time affected the adsorption of Pb^{2+} onto unmodified and modified *C. sieberiana* seed differently and shows that the modification increased the efficiency of adsorption. The Langmuir isotherm model and pseudo-second-order models best explain the adsorption mechanism involved in the uptake of Pb^{2+} by the adsorbents which suggest chemosorption. The adsorption was very fast as more than 75% were removed from the solution within 40 min. The overall adsorption process was controlled by one or more steps such as external diffusion, pore diffusion, surface diffusion and adsorption on the pore surface or a combination of more than one step. This study showed that *C. sieberiana* seed could be utilized as effective low-cost adsorbents for metal ions.

Symbols

q_e — Adsorption capacity of the adsorbents
C_0 — Initial metal ion concentration in solution
C_e — Equilibrium of the metal ion concentration
V — Volume of adsorbate
m — Mass of the adsorbent
q_t — Amounts of metal ions adsorbed at time t and
q_e — Amounts of metal ions adsorbed at equilibrium
K_1 — Pseudo-first-order adsorption rate constant
K_2 — Equilibrium rate constant of pseudo-second-order adsorption
h — Initial sorption rate
q_t — Adsorption at time t
K_{id} — Intraparticle diffusion rate constant
C — Constant that gives the thickness of the boundary layer
$q_{e,exp}$ — Experimental equilibrium adsorption capacity
$q_{e,cal}$ — Theoretical equilibrium adsorption capacity
n — Number of experimental data points
p — Number of parameters in each isotherm model.
K_L — Langmuir adsorption constant related to the energy of adsorption
q_m — Maximum monolayer adsorption capacity of the adsorbent
K_F — Freundlich adsorption constant related to the adsorption capacity
n — Adsorption intensity of the adsorbents
T — Temperature
R — Ideal gas constant
B — Temkin constant related to the heat of adsorption or the maximum binding energy

References

[1] N. Zhang, G.-L. Zang, C. Shi, H.-Q. Yu, G.-P. Sheng, A novel adsorbent TEMPO-mediated oxidized cellulose nanofibrils modified with PEI: preparation, characterization, and application for Cu(II) removal, J. Hazard. Mater., 316 (2016) 11–18.

[2] J.J. Li, L.L. Xiao, S.L. Zheng, Y.C. Zhang, M. Luo, C. Tong, H.D. Xu, Y. Tan, J. Liu, O. Wang, F.H. Liu, A new insight into the strategy for methane production affected by conductive carbon cloth in wetland soil: beneficial to acetoclastic methanogenesis instead of CO_2 reduction, Sci. Total Environ., 643 (2018) 1024–1030.

[3] S.R. Shukla, R.S. Pai, Adsorption of Cu(II), Ni(II) and Zn(II) on modified jute fibres, Bioresour. Technol., 96 (2005) 1430–1438.

[4] D.P. Facchi, A.L. Cazetta, E.A. Canesin, V.C. Almeida, E.G. Bonafé, M.J. Kipper, A.F. Martins, New magnetic chitosan/alginate/Fe_3O_4@SiO_2 hydrogel composites applied for removal of Pb(II) ions from aqueous systems, Chem. Eng. J., 337 (2018) 595–608.

[5] J.O. Esalah, M.E. Weber, J.H. Vera, Removal of lead, cadmium and zinc from aqueous solutions by precipitation with sodium di-(*n*-octyl) phosphinate, Can. J. Chem., 78 (2000) 948–954.

[6] V. de A. Cardoso, A.G. de Souza, P.P.C. Sartoratto, L.M. Nunes, The ionic exchange process of cobalt, nickel and copper(II) in alkaline and acid-layered titanates, Colloids Surf., A, 248 (2004) 145–149.

[7] D. Buerge-Weirich, R. Hari, H. Xue, P. Behra, L. Sigg, Adsorption of Cu, Cd, and Ni on goethite in the presence of natural groundwater ligands, Environ. Technol., 36 (2002) 328–336.

[8] L. Xia, Z.H. Huang, L. Zhong, F.W. Xie, C.Y. Tang, C.P. Tsui, Bagasse cellulose grafted with an amino-terminated hyperbranched polymer for the removal of Cr(VI) from aqueous solution, Polymer, 10 (2018) 391–405.

[9] G. Xu, L. Wang, Y. Xie, M.L. Tao, W.Q. Zhang, Highly selective and efficient adsorption of Hg^{2+} by a recyclable aminophosphonic acid functionalized polyacrylonitrile fiber, J. Hazard. Mater., 344 (2018) 679–688

[10] I. Ali, M. Asim, T.A. Khan, Low cost adsorbents for the removal of organic pollutants from wastewater, J. Environ. Manage., 113 (2012) 170–183.

[11] S.E. Bailey, T.J. Olin, R.M. Bricka, D.D. Adrian, A review of potentially low-cost sorbents for heavy metals, Water Res., 33 (1999) 2469–2479.

[12] H.O. Abugu, P.A.C. Okoye, V.I.E. Ajiwe, P.C. Oford, Preparation and characterisation of activated carbon from agrowastes peanut seed (*African canarium*) and palm kernel shell, Int. J. Innovative Res. Dev., 3 (2014) 13.

[13] S. Vitas, T. Keplinger, N. Reichholf, R. Figi, E. Cabane, Functional lignocellulosic material for the remediation of copper(II) ions from water: towards the design of a wood filter, J. Hazard. Mater., 355 (2018) 119–127.

[14] A. Saeed, M.W. Akhter, M. Iqbal, Removal and recovery of heavy metals from aqueous solution using papaya wood as a new biosorbent, Sep. Purif. Technol., 45 (2005) 25–31.

[15] N.A.A. Babarinde, J.O. Babalola, R.A. Sanni, Biosorption of lead ions from aqueous solution by maize leaf, Int. J. Phys. Sci., 1 (2006) 23–26.

[16] M. Šćiban, M. Klašnja, Wood sawdust and wood originate materials as adsorbents for heavy metal ions, Holz als Roh- und Werkstoff, 62 (2004) 69–73.

[17] P.D. Johnson, M.A. Watson, J. Brown, I.A. Jefcoat, Peanut hull pellets as a single use sorbent for the capture of Cu(II) from wastewater, Waste Manage., 22 (2002) 471–480.

[18] H.O. Abugu, P.A.C. Okoye, V.I.E. Ajiwe, P.E. Omuku, U.C. Umeobika, Preparation and characterization of activated carbon produced from oil bean (Ugba or Ukpaka) and snail shell, J. Environ. Anal. Chem., 2 (2015) 165, doi: 10.4172/2380-2391.1000165.

[19] O.C. Ugwoke, B. Dauda, J.A. Ezugwu, H.O. Abugu, L.O. Alum, S.I. Eze, O.A. Odewole, Chromium adsorption using modified locust bean and maize husk, Der Pharma Chem., 12 (2020) 7–14.

[20] B. Chen, H. Zhao, S.J. Chen, F.X. Long, B.Q. Huang, B.Q. Yang, X.J. Pan, A magnetically recyclable chitosan composite adsorbent functionalized with EDTA for simultaneous capture of anionic dye and heavy metals in complex wastewater, Chem. Eng. J., 356 (2019) 69–80.

[21] N. Supanchaiyamat, K. Jetsrisuparb, J.T.N. Knijnenburg, D.C.W. Tsang, A.J. Hunt, Lignin materials for adsorption: current trend, perspectives and opportunities, Bioresour. Technol., 272 (2019) 570–581.

[22] M. Sćiban, M. Klasnja, B. Skrbić, Modified softwood sawdust as adsorbent of heavy metal ions from water, J. Hazard. Mater., 136 (2006) 266–271.

[23] Q. Li, J.P. Zhai, W.Y. Zhang, M.M. Wang, J. Zhou, Kinetic studies of adsorption of Pb(II), Cr(III) and Cu(II) from aqueous solution by sawdust and modified peanut husk, J. Hazard. Mater., 141 (2006) 163–167.

[24] C.R.T. Tarley, S.L.C. Ferreira, M.A.Z. Arruda, Use of modified rice husks as a natural solid adsorbent of trace metals: characterization and development of an on-line preconcentration system for cadmium and lead determined by FAAS, Microchem. J., 77 (2004) 163–175.

[25] K.J. Tiemann, G. Gamez, K. Dokken, J.G. Parsons, J.L. Gardea-Torresdey, Chemical modification and X-ray absorption studies for lead(II) binding by *Medicago sativa* (*alfalfa*) biomass, Microchem. J., 71 (2002) 287–293.

[26] K.S. Low, C.K. Lee, A.C. Leo, Removal of metals from electroplating wastes using banana pith, Bioresour. Technol., 51 (1995) 227–231.

[27] O. Karnitz Jr., L.V.A. Gurgel, J.C.P. de Melo, V.R. Botaro, T.M.S. Melo, R.P. de Freitas Gil, L.F. Gil, Adsorption of heavy metal ion from aqueous single metal solution by chemically modified sugarcane bagasse, Bioresour. Technol., 98 (2007) 1291–1297.

[28] M.A. Ferro-García, J. Rivera-Utrilla, J. Rodriguez-Gordillo, I. Bautista-Toledo, Adsorption of zinc, cadmium, and copper

on activated carbons obtained from agricultural by-products, Carbon, 26 (1988) 363–373.
[29] A.A. Olapade, O.A. Ajayi, I.A. Ajayi, Physical and chemical properties of *Cassia sieberiana* seeds, Int. Food Res. J., 21 (2014) 767–772.
[30] S. Lagergren, About the theory of so-called adsorption of soluble substances, Kungliga Svenska Vetenskapsakademiens Handlingar, 24 (1898) 1–39.
[31] Y.S. Ho, G. McKay, Pseudo-second order model for sorption processes, Process Biochem., 34 (1999) 451–465.
[32] Y.S. Ho, G. McKay, The kinetics of sorption of basic dyes from aqueous solution by sphagnum moss peat, Can. J. Chem. Eng., 76 (1998) 822–827.
[33] W.J. Weber, J.C. Morris, Kinetics of adsorption on carbon from solution, J. Am. Soc. Civ. Eng., 89 (1963) 31–60.
[34] A. Kapoor, R.T. Yang, Correlation of equilibrium adsorption data of condensible vapours on porous adsorbents, Gas Sep. Purif., 3 (1989) 187–192.
[35] D.W. Marquardt, An algorithm for least-squares estimation of non-linear parameters, J. Soc. Ind. Appl. Math., 11 (1963) 431–441.
[36] M.K. Miyittah, F.W. Tsyawo, K.K. Kumah, C.D. Stanley, J.E. Rechcigl, Suitability of two methods for determination of point of zero charge (PZC) of adsorbents in soils, Commun. Soil Sci. Plant Anal., 47 (2016) 101–111.
[37] G. Uehara, G. Gillman, The Mineralogy, Chemistry, and Physics of Tropical Soils with Variable Charge Clays, Westview Press Inc., Boulder, Colorado, 1981.
[38] B.Y. Nale, J.A. Kagbu, A. Uzairu, E.T. Nwankwere, S. Saidu, H. Musa, Kinetic and equilibrium studies of the adsorption of lead(II) and nickel(II) ions from aqueous solutions on activated carbon prepared from maize cob, Der Chem. Sin., 3 (2012) 302–312.
[39] J.Y. Zheng, Q.L. Zhao, Z.F. Ye, Preparation and characterization of activated carbon fiber (ACF) from cotton woven waste, Appl. Surf. Sci. J., 299 (2014) 86–91.
[40] D.V. Bojić, M.S. Ranđelović, A.R. Zarubica, J.Z. Mitrović, M.D. Radović, M.M. Purenović, A.L. Bojić, Comparison of new biosorbents based on chemically modified *Lagenaria vulgaris* shell, Desal. Water Treat., 51 (2013) 6871–6881.
[41] J.J. Liu, X.C. Wang, B. Fan, Characteristics of PAHs adsorption on inorganic particles and activated sludge in domestic wastewater treatment, Bioresour. Technol., 102 (2011) 5305–5311.
[42] X. Hu, J.C. Cao, H.Y. Yang, D.H. Li, Y. Qiao, J.L. Zhao, Z.X. Zhang, L. Huang, Pb^{2+} biosorption from aqueous solutions by live and dead biosorbents of the hydrocarbon-degrading strain *Rhodococcus* sp. HX-2, PLoS One, 15 (2020) e0226557, https://doi.org/10.1371/journal.pone.0226557.
[43] J.D. Roberts, M.C. Caserio, Basic Principles of Organic Chemistry and Modern Organic Chemistry, California Institute of Technology, W.A. Benjamin, Inc. , Menlo Park, CA, 1977.
[44] P. Kumar Jha, V. Kumar Jha, Iodine adsorption characteristics of activated carbon obtained from *Spinacia oleracea* (spinach) leaves, Mongolian J. Chem., 21 (2020) 1–11, doi: 10.5564/mjc.v21i47.1249.
[45] G. Kirova, Z. Velkova, V. Gochev, Copper(II) removal by heat inactivated *Streptomyces fradiae* biomass: surface chemistry characterization of the biosorbent, J. BioSci. Biotech., (2012) 77–82.
[46] H.R. Hesas, A. Arami-Niya, W.M.A.W. Daud, J.N. Sahu, Preparation and characterization of activated carbon from apple waste by microwave-assisted phosphoric acid activation: application in methylene blue adsorption, Bioresources, 8 (2013) 2950–2966.
[47] G.F. de Oliveira, R.C. de Andrade, M.A.G. Trindade, H.M.C. Andrade, CT. de Carvalho, Thermogravimetric and spectroscopic study (TG–DTA/FTIR) of activated carbon from the renewable biomass source babassu, Quim. Nova, 40 (2017) 284–292.
[48] A. Bazan, P. Nowicki, P. Półrolniczak, R. Pietrzak, Thermal analysis of activated carbon obtained from residue after supercritical extraction of hops, J. Therm. Anal. Calorim., 125 (2016) 1199–1204.
[49] V.K. Gupta, M. Gupta, S. Sharma, Process development for the removal of lead and chromium from aqueous solutions using red mud—an aluminium industry waste, Water Resour., 35 (2001) 1125–1134.
[50] B. Das, N.K. Mondal, Calcareous soil as a new adsorbent to remove lead from aqueous solution: equilibrium, kinetic and thermodynamic study, Univ. J. Environ. Res. Technol., 1 (2011) 515–530.
[51] M.E. Argun, S. Dursun, C. Ozdemir, M. Karatas. Heavy metal adsorption by modified oak sawdust: thermodynamics and kinetics, J. Hazard. Mater., 141 (2007) 77–85.
[52] S. Swapna Priya, K.V. Radha, Equilibrium, isotherm, kinetic and thermodynamic adsorption studies of tetracycline hydrochloride onto commercial grade granular activated carbon, Int. J. Pharm. Sci., 71 (2014) 42–51.
[53] S. Rangabhashiyam, N. Anu, M.S. Giri Nandagopal, N. Selvaraju, Relevance of isotherm models in biosorption of pollutants by agricultural byproducts, J. Environ. Chem. Eng., 6 (2014) 2398–2414.
[54] A.O. Dada, A.P. Olalekan, A.M. Olatunya, O. Dada, Langmuir, Freundlich, Temkin and Dubinin–Radushkevich isotherms studies of equilibrium sorption of Zn^{2+} onto phosphoric acid modified rice husk, J. Appl. Chem., 3 (2012) 2278–5736.
[55] J. Sreńscek-Nazzal, U. Narkiewicz, A.W. Morawski, R. Wróbel, A. Gęsikiewicz-Puchalska, B. Michalkiewicz, Modification of commercial activated carbons for CO_2 adsorption, Acta Phys. Pol. A, 129 (2016) 394–401.
[56] B. Singha, S.K. Das, Adsorptive removal of Cu(II) from aqueous solution and industrial effluent using natural/agricultural wastes, Colloids Surf., B, 107 (2013) 97–106.
[57] E. Cristiano, Y.-J. Hu, M. Sigfried, D. Kaplan, H. Nitsche, A comparison of point of zero charge measurement methodology, Clays Clay Miner., 59 (2011) 107–115.
[58] M. Kosmulski, Attempt to determine pristine points of zero charge of Nb_2O_5, Ta_2O_5, and HfO_2, Langmuir, 13 (1997) 6315–6320.
[59] J.W. Moon, H.L. Lee, J.D. Kim, G.D. Kim, D.A. Lee, H.W. Lee, Preparation of ZrO_2-Coated NiO powder using surface-induced coating, Mater. Lett., 38 (1999) 214–220.
[60] T. Mahmood, M.T. Saddique, A. Naeem, P. Westerhoff, S. Mustafa, A. Alum, Comparison of different methods for the point of zero charge determination of NiO, Ind. Eng. Chem. Res., 50 (2011) 10017–10023.
[61] K. Mohanty, M. Jha, B.C. Meikap, M.N. Biswas, Biosorption of Cr(VI) from aqueous solutions by *Eichhornia crassipes*, Chem. Eng. J., 117 (2006) 71–77.